nature sustainability

Analysis

https://doi.org/10.1038/s41893-024-01450-3

Landscape patterns in stand-replacing disturbances across the world's forests

Received: 25 October 2023

Accepted: 24 September 2024

Published online: 15 November 2024

Check for updates

Nezha Acil[1,2,3,4] ✉, Jonathan P. Sadler[1,2], Cornelius Senf[5], Susanne Suvanto[1,2,6] & Thomas A. M. Pugh[1,2,7]

The spatial imprint of forest disturbances, which can result from a variety of anthropogenic and natural causes, is important in shaping the form and function of the world's forests. However, we lack a systematic assessment of how the forms of forest disturbances differ globally, which could help in sustainable forest policy and management initiatives to protect forest biomes. Here we produce a global-scale quantification of disturbance patch structures. Using indicators of magnitude, complexity and context, we found that the forms of stand-replacing disturbances can be classified into four broad patterns, whose spatial dominance varies across regions. Human activities were shown to introduce disturbance structures that are not naturally common, especially in the tropics. The consistency of these patterns across biomes outside intact forests suggests that a continuation of current dynamics may lead to a structural homogenization of the world's forests, with potential consequences for forest ecology and functions. These results provide a greater understanding of the mechanisms governing forest dynamics and elucidating the causal agents of disturbances. This will be a key step towards building more reliable projections of future forest conditions, informing policymaking and ensuring the sustainability of forest management.

Stand-replacing disturbances are natural or anthropogenic events that cause the sudden death of a group of trees[1–3]. These events occur at different frequencies and intensities and are generally temporary, forming an integral part of the natural cycle of forest dynamics[2]. The patches left by disturbances also vary greatly in terms of size, shape and spatial arrangement. These patterns of damage are the result of a complex combination of factors, involving the disturbance agents, the state of the forest and the broader environmental context[4]. Because tree growth and succession happen over timescales of decades to centuries, disturbance patterns have a long-lasting impact on forest structure and composition[4,5], with consequent impacts on both carbon cycling[6] and habitat diversity[7]. The latter, in turn, is then crucial for the diversity and abundance of fauna and flora[8,9]. Understanding disturbance dynamics is therefore a fundamental building block for understanding the form and function of the world's forests.

While a growing body of works focuses on characterizing disturbance rates at a large scale[3,10–13], work on characterizing the structure of disturbances has generally been limited to the landscape or regional scales[14–16]. The few studies that have assessed structural patterns over the scale of one or more biomes have reported substantial consistency in the shapes and sizes of disturbance patches between unmanaged forests in temperate and boreal biomes, but with large variations within biomes[17,18]. Whether such consistency holds more broadly across biomes, particularly given management pervasiveness[19,20], remains unknown.

[1]School of Geography, Earth and Environmental Sciences, University of Birmingham, Birmingham, UK. [2]Birmingham Institute of Forest Research, University of Birmingham, Birmingham, UK. [3]Institute for Environmental Futures, School of Geography, Geology and the Environment, University of Leicester, Leicester, UK. [4]National Centre for Earth Observation, University of Leicester, Leicester, UK. [5]School of Life Sciences, Earth Observation for Ecosystem Management, Technical University of Munich, Freising, Germany. [6]Natural Resources Institute Finland (Luke), Helsinki, Finland. [7]Department of Physical Geography and Ecosystem Science, Lund University, Lund, Sweden. ✉e-mail: nezha.acil@live.com

Several mechanisms affect the structure of disturbance patches. The nature of a disturbance agent and its intensity can fundamentally influence the form of the marks left on forest landscapes. For example, rapidly and linearly moving processes, such as tornadoes or flooding, may produce patches that are elongated or linearly arranged[14,21–24]. By contrast, an enduring contagion process, such as a biotic outbreak or a smouldering fire, would result in patches that are growing over time, clumped or coalescent[25,26], whereas industrial clear-cutting may produce patches that have compact geometries and regular sizes and patterns[8].

In addition to the causal agent, the local environment also plays a major role in shaping disturbance patches. Climate, weather and topography can strongly modulate the formation process of individual patches. For example, dry windy conditions may lead to stretched burn scars, while steep slopes may favour downslope flows and mass movements[27]. Forest properties, such as tree health and species composition, also influence the propagation of the disturbance process. For example, the speed of a fire spreading may vary depending on tree flammability traits[28], while trees collectively subjected to a stress would be weakened and thus more vulnerable to disease outbreaks[29]. Finally, disturbance patches may simply reflect the shape and configuration of the original forest fragment, which is the case for degraded or land-use-fragmented forests[30,31]. While links between forest composition and disturbance agent suggest a link between disturbance patch structure and biomes, other factors suggest a more subtle variation of disturbance patch structure following the physical environment and local management norms.

The structure of disturbance patches has fundamental implications for forest recovery and the biodiversity supported. Complex or elongated patches increase edge effect, thus forest exposure to the altered microclimates inside the patch and permeability for other species[32,33]. Recolonization from the surrounding forest can be fast in smaller patches, while it may be slowed down in larger ones, owing to longer distances to seed sources and altered microclimatic conditions inside the patches[4,34,35]. Depending on forest types, these differences in conditions can be expected to influence the successional trajectory[34,35]. Clusters of small patches within a closed-canopy forest affect habitat quality by deteriorating the physical conditions required by shade-tolerant and forest interior specialists[36,37], whereas with larger patches, they may create substantial barriers to habitat connectivity, impeding species movements, while also staging the way for fragmentation or degradation processes[38]. Identifying such structural characteristics in disturbances across the world opens the door for a better understanding of the biogeography of a broad range of species, communities and ecological processes, which is the very basis for constructing sustainable action plans for forests.

In this study, we used a Landsat-based tree cover loss data (Global Forest Change (GFC))[10] and a selection of established and novel metrics describing patch structure in terms of magnitude, complexity and context (Table 1) to categorize and map major patterns in forest disturbances wall to wall across the world and over the period 2002–2014, when the tree cover loss data were the most consistent (Supplementary Fig. 3). We sought to (1) identify the most prominent disturbance patterns, (2) explore their distribution across biomes and potential linkages with underlying drivers and (3) address the effects of human activities on disturbance patterns, contrasting such effects across biomes. We define as forest disturbance any loss in tree cover identifiable by remote sensing at 30 m resolution, where the land is assumed to remain a forest. The definition focuses on disturbances as temporary events, excluding large land use changes (>300 m resolution pixels, that is, 9 ha, from European Space Agency Climate Change Initiative (ESA CCI) Land Cover data[39]), but including anthropogenic activities (that is, harvest and shifting agriculture). Disturbances occurring after the loss reported in the GFC data are ignored, as the vegetation cover is assumed not to contain mature trees (that is, only the spatial characteristics of the first disturbance event are considered). Our definition of forest includes open-canopy forests and woodlands where tree cover can be below 10%.

Statistics of disturbance patch metrics at the global scale

Between 2002 and 2014, we identified 249,149,911 patches aligning with our definition of forest disturbances. The magnitude of disturbance patches, represented by mean area and count of years (Table 1), peaks in Sweden, Finland, western Russia, southeastern Asia, southeastern Amazon and northwestern and southeastern United States (Supplementary Fig. 4). However, patch areas remain small in most of the African continent. Complexity metrics, represented by mean shape and elongation indices, consistently indicate more complex structures in the aforementioned regions, along with central Africa. Context metrics, reflected by spatio-temporal clustering within a 5 km buffer, show that disturbance patches tend to be spatially clustered in Siberia, Africa, southeastern Asia and parts of the Amazon and Canada. Disturbances also appear less temporally clustered in Europe, western Russia, southeastern Asia, northwestern and eastern United States, eastern Amazon and central and western Africa than in other parts of the world.

Four disturbance patterns identified globally

Grouping of the 2002–2014 disturbance patches using *k*-means clustering[40] revealed four distinct disturbance structures across the world (Table 2). The patterns identified correspond to (1) small-isolated patches, characterized by the smallest mean areas (mean = 0.20 ha, that is, ~2 pixels), and the lowest spatio-temporal clustering (mean = 88.69 concomitant patches within 5 km and accounting for 8% of the disturbance area during the period studied); (2) clustered patches, which are the most spatiotemporally clustered (mean = 386.16 concomitant patches within 5 km and 50% of the disturbance area over the period studied); (3) complex patches, which are of medium size (mean = 1.17 ha) and complex, with the most stretched shapes (mean = 0.66 for the elongation index); and (4) large-multiyear patches, which are the largest (mean = 9.40 ha), the most long-lasting (mean = 2.12 years) and also the most complex (mean = 1.86 in shape index).

There was a remarkable consistency across biomes in the relative composition of the different disturbance patterns in terms of counts (Fig. 1a). Only the Tundra biome diverged markedly, with a much higher relative frequency of clustered patches, reflecting the very sparse woody cover in this region. This corroborates and extends previous conclusions that found little difference in disturbance characteristics between boreal and temperate biomes[17]. However, there were very large differences in the total area affected by each disturbance pattern, with large-multiyear patterns dominating disturbed areas in the boreal and Mediterranean regions, whereas complex and large-multiyear patterns contributed roughly equally to areas affected in tropical and temperate biomes (Fig. 1b). Small-isolated patches are the most prevalent globally comprising between 56% and 70% of patches across all biomes (Fig. 2a). Overall, they account for 62.90% of the total number of patches, but collectively represent only 12.94% of the global forest area disturbed (Table 1 and Supplementary Figs. 8 and 9). They dominate by their total areas in the arctic regions, as well as in some mountain ranges, such as the Himalayas, the Scandinavian mountains and central Madagascar (Fig. 2a and Supplementary Fig. 9). They are also dominant in tropical forest areas, in parts of the Amazon, Africa and central Borneo Island.

Clustered patches form a minority in terms of counts (8.55% of the total number of patches) and coverage (3.39% of the total area disturbed) (Table 1, Fig. 2a, and Supplementary Figs. 8 and 9). They are characteristically present along transitional zones with drylands, notably with the African Sahara, the deserts of central Australia, the grasslands of central North America and the tundra of northmost Canada and eastern Russia. Clustered patches also appear in the remote

https://doi.org/10.1038/s41893-024-01450-3

Table 1 | Disturbance patch metrics selected to characterize the structure of disturbances (values rounded to two decimal places)

Class	Metric	Description	Unit	Theoretical range	Statistics for the disturbance patches					
					Mean	s.d.	Minimum	Maximum	1st percentile	99th percentile
Magnitude	Growth (count of years)	Number of years over which the patch showed continuous growth	Years	≥1	1.07	0.28	1.00	8.00	1	3
	Area	Patch area	ha	>0	1.08	60.43	0.09	221,025.49	0.09	12.06
Shape	Shape index	Indicates the complexity of the patch shape, with increasing values indicating increasing complexity	Unitless	≥1	1.20	0.41	0.98	142.88	0.98	2.71
	Elongation	The extent to which a patch adopts a linear (1) or circular (0) form	Unitless	[0,1[	0.49	0.13	0.00	1.00	0.36	0.81
Context	Spatial clustering	Number of concomitantly occurring surrounding patches within a 5 km radius from the centroid of the focal patch, reflecting whether a patch is isolated or part of a cluster	Patches	≥0	120.08	141.69	0.00	4,155	2	667
	Temporal clustering	Percentage of total area disturbed within a 5 km radius from the centroid of the focal patch, which occurred within a single year, reflecting whether forest loss is pulsatile or steady over time	%	>0	12%	16%	0%	100%	2%	92%

Full descriptions of metrics are provided in Supplementary Table 1.

and intact forests of the Amazon. Intact forests are defined as large forest fragments of more than 50,000 ha, assumed to be minimally influenced by human activities[41].

Complex patches are substantial both in terms of counts (22.58% of the total number of patches) and area (26.84% of the total area disturbed) (Table 1, Fig. 2a, and Supplementary Figs. 8 and 9). Like the small-isolated patches, they are ubiquitous, with a spatial dominance in human-influenced regions, notably in northern Europe, China, southeastern Asia, southeastern United States and southeastern Amazon.

Finally, large-multiyear patches, although relatively rare in number (5.96%), account for most of the disturbed areas globally (56.83%) (Table 1, Fig. 2a, and Supplementary Figs. 8 and 9). They represent typically 2.5–6.5% of the total number of patches in each biome and are prevalent in regions affected by large wildfires, notably in fire-prone boreal Canada and Siberia. They are also concentrated in regions subject to human activities, where they co-dominate with the complex patches, notably throughout southeastern Amazon, Southeast Asia and the United States, and central Chile.

Large variability within biomes

Although at the scale of biomes, the relative frequency of the different patch structures was consistent within most biomes, we found marked variability in their spatial distribution (Fig. 2a), as well as the diversity of the pattern types found (Fig. 2b). This variability showed clear spatial consistency, indicating that it is not simply a result of the 13 year period of not sufficiently sampling rare disturbance events. Some of the patterns in Fig. 2a are consistent with known areas of strong human influence. For instance, the large-multiyear patches dominating in Indonesia and Malaysia, which mark them out from the rest of the tropics, are consistent with the locations of oil palm and rubber plantations in these countries[42,43]. Similarly, the abundance of small-isolated patches in England is probably linked to the highly fragmented forest landscape limiting patch size[44,45]. The diversity of disturbance patterns, estimated with the Shannon diversity index[46] based on cover area, presents marked hotspots across the world. This is particularly visible in many parts of Africa, including the western coasts of Madagascar (Fig. 2b), which suggests a more uneven distribution of disturbance patterns compared with other continents. This may be explained by the distribution of the clustered and large-multiyear patches (Supplementary Figs. 8 and 9) and the smaller areas and shorter perimeters observed in disturbances there (Supplementary Fig. 4). China, Portugal, central and northern Europe, Central America and eastern Brazil also emerge as areas of high diversity. Overall, the biome appears to be a poor indicator for disturbance patch characteristics. We speculate that the physical environment of the forest; the type, intensity and legacy of human influence; and the traits of the species found there (as filtered by their history) may instead be the driving patterns of the current biogeography of disturbance.

Linkages with potential underlying drivers

The association of disturbance patterns with existing global databases on environmental conditions and human activities provides some insights into the drivers of these patterns. In high latitudes and elevations, between the lower timberline and the tree line, our definition of forests is represented by scattered small groups of trees subsisting under the harsh conditions characterizing these environments. The small and isolated disturbance patterns prevailing in these regions may reflect the size of the isolated tree stands that can be found there (Supplementary Fig. 8). Small-isolated patterns also predominate in some intact closed-canopy forests in the Amazon where the effects of human activities and fragmentation are assumed to be minimal (Figs. 2a and 3, and Supplementary Fig. 12b). This underpins the rarity of large disturbances in these forests and highlights the importance of small-scale gap dynamics that drive natural canopy turnover there[47,48]. These gaps are punctual, caused by small-scale events (for example, blowdowns) that result in openings in the otherwise continuous canopy.

https://doi.org/10.1038/s41893-024-01450-3

Table 2 | Statistics of the metrics by the disturbance patterns identified with unsupervised clustering (values rounded to two decimal places)

Cluster label	Patch count (*n*)	Total areas (Mha)	Mean count of years±1 s.d.	Mean area (ha)±1 s.d.	Mean shape index±1 s.d.	Mean elongation index±1 s.d.	Mean spatial clustering (count)±1 s.d.	Mean temporal clustering (%)±1 s.d.
Small-isolated	156,722,592 (62.90%)	31.81 (12.94%)	1.00±0.00	0.20±0.58	1.03±0.07	0.41±0.06	88.69±83.69	8%±0.08
Clustered	21,313,772 (8.55%)	8.33 (3.39%)	1.01±0.10	0.39±1.74	1.14±0.29	0.47±0.12	386.16±260.63	50%±0.27
Complex	56,257,656 (22.58%)	65.97 (26.84%)	1.00±0.00	1.17±3.56	1.52±0.35	0.66±0.07	103.58±96.11	9%±0.09
Large-multiyear	14,855,891 (5.96%)	139.70 (56.83%)	2.12±0.35	9.40±242.05	1.86±0.95	0.64±0.11	122.10±128.67	11%±0.14

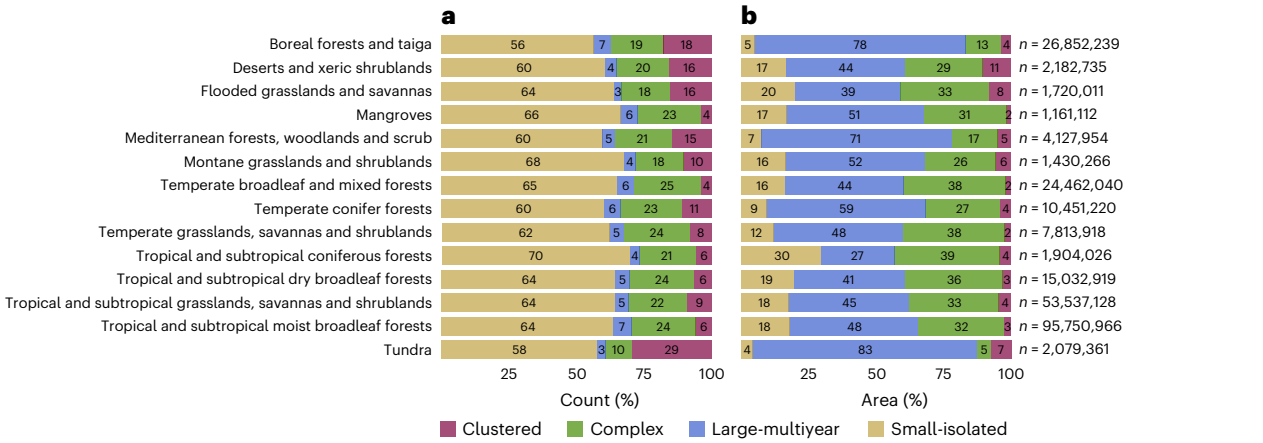

Fig. 1 | Proportion of disturbance patterns by biome based on count and area disturbed. a, In terms of counts, the prevalence of the patterns remains similar across most biomes, with the small-isolated pattern having the largest fraction. The complex pattern is the second most prevalent, except in the tundra biome where it is exceeded by the clustered pattern. The large-multiyear pattern is the least prevalent, except in mangroves, temperate broadleaf and mixed forests, and tropical moist broadleaf forests, where it exceeds the fraction of the clustered pattern. **b**, In terms of total area, substantial variability appears across biomes, although the largest fraction remains taken by the large-multiyear pattern. The only exception is in the tropical coniferous biome, where the complex pattern has a greater fraction.

It should be noted that small-isolated patches often correspond to single pixels from the original tree cover loss data. The commission and omission errors associated with these pixels[49] suggest that there may be overestimations of the small-isolated patches in the temperate and boreal forests (almost the double of false negatives, as false positives represent 11.8% in the temperate biome and 12.0% in the boreal biome, while false negatives represent 6.1% in both biomes) and possible underestimations in the tropical biome (13.0% for false positives and 16.9 for false negatives). While single-pixel events could be partially caused by classification noise, their clear and coherent spatial variation, aligning with our knowledge of forest disturbances across regions, suggests that the signal may be more than just noise and that any such noise has a minimal influence on the overall patterns we identify.

The dominance of clustered patches in large areas of the intact contiguous forests of the Amazon (Figs. 2a and 3, and Supplementary Fig. 12b) is consistent with the blowdown and drought-related mortality, which are known to be major agents of disturbance there[50,51]. Wind can damage multiple nearby locations at the same time, while drought impacts are strongly mediated by small-scale variations in water availability[52], thus generating the clustered pattern, which has been suggested to be broadly associated with natural disturbances[16,53,54]. Clustered patches are also prominent throughout the ecotones with drylands, parts of the Mediterranean regions and in the boreal peatlands (Fig. 2a). They also show a substantial association with fire (Fig. 4). Forests in these regions are fragmented and often disturbed by large wildfires[55]. The clustered patch structure may reflect such fires spreading in sparsely wooded landscapes with many disconnected stands. The occurrence of clustered patches within the intact forests of the tropics (Figs. 2a and 3, and Supplementary Fig. 12) and their overall association with a higher forest landscape integrity index, an indicator of human influence on forest landscapes[56] (Supplementary Fig. 11), suggest that these patterns are probably more commonly the results of natural processes, rather than anthropogenic activities.

Complex patches predominate in temperate and tropical regions where human activities are prevalent (Fig. 2a and Supplementary Fig. 13). This is particularly visible in areas where tree farming, urbanization and shifting agriculture are occurring (Fig. 4 and Supplementary Fig. 13). The link with human activities is also supported by the association with lower values in the forest integrity index (Supplementary Fig. 11). Although forestry, perhaps the most common anthropogenic disturbance, is often associated with simple geometries, such as a square or a rectangle, the high complexity measured may be the result of intricate and/or interconnected patches that complicate the shapes (for example, dendritic and fishbone patterns taken by deforestation in the Amazon; elongated rectangles of harvesting in Poland; checkerboard pattern of clear-cutting in Russia; linear features, such as roads and tracks carved within forests; and where the density of different activities may lead to intricate shapes).

Large-multiyear patches are mainly found in boreal and Mediterranean regions in association with fires and outside intact forests in the tropics, in areas dominated by harvest (Figs. 1, 2a, 3 and 4, and Supplementary Fig. 12). Notable regions include western North America, where harvest is mixed with fire and biotic outbreaks; southeast North America, where harvest is combined with hurricanes[57]; and tropical Southeast Asia and the southeastern Amazon where fire is used for forest clearing[58]. They may also be associated with regions where patch detection may be limited by cloud obstruction, generating an erroneous multiyear composition (for example, tropical cloud forests).

https://doi.org/10.1038/s41893-024-01450-3

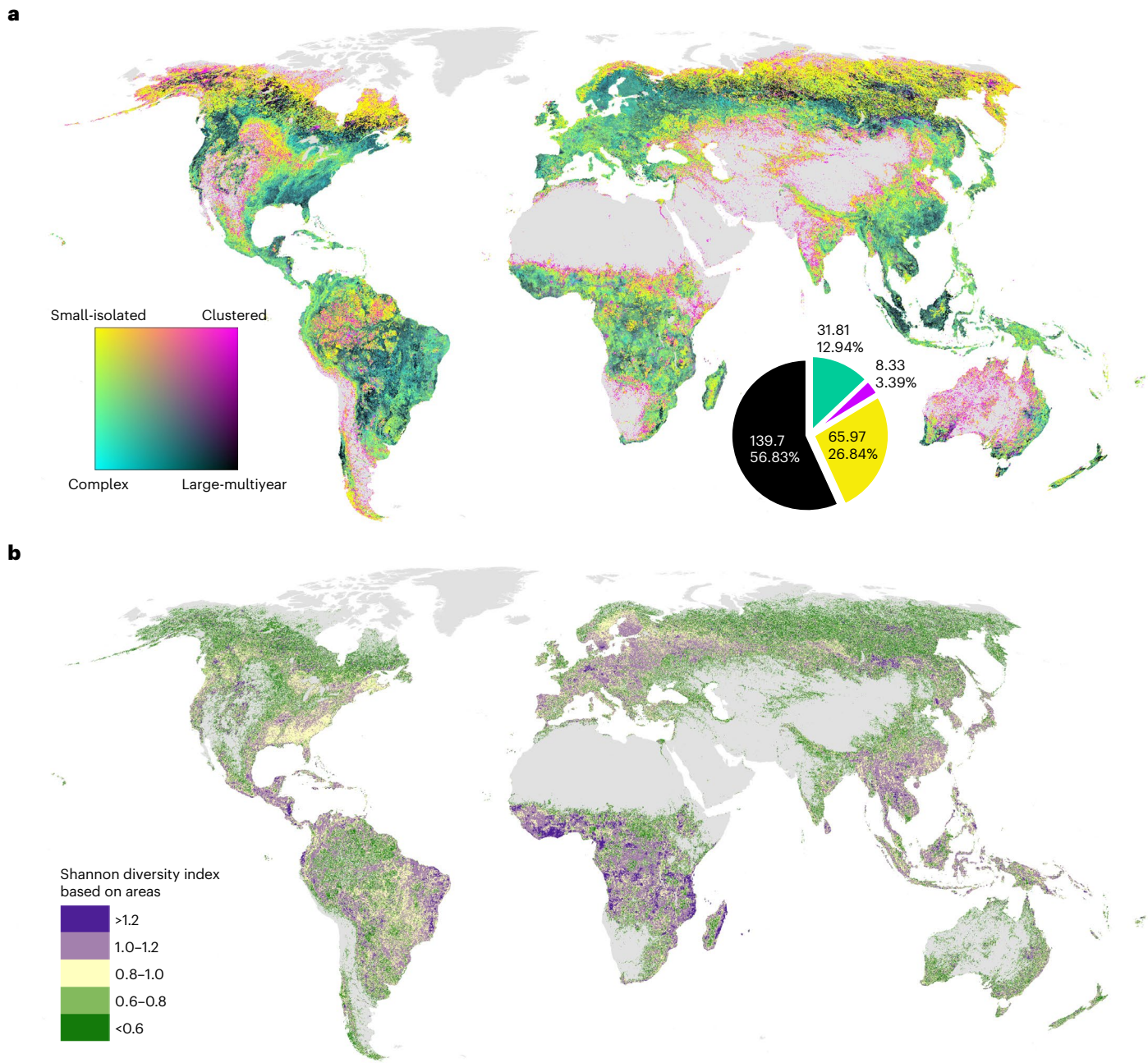

Fig. 2 | Distribution of disturbance patterns based on total areas covered. **a**, Relative importance of disturbance patterns. To reflect the contribution of each patch type within a grid cell based on areal dominance, we used a cyan–magenta–yellow–key (black) colour scheme (CMYK), with the percentage of each patch type added as a percentage of colour in the CMYK space. We used black for large-multiyear, cyan for complex, magenta for clustered and yellow for small-isolated patterns. No forest mask is applied. **b**, Shannon diversity index in disturbance patterns based on cover percentage. No forest mask is applied. Most of Africa is characterized by a high diversity index compared with other regions.

Multiyear patches may also reflect natural long-term processes, possibly biotic spreading[25,26] and cascading effects from wind or wildfire[59].

Implications for forest ecosystems

Our global geography of disturbance patch structure provides insights into how forests are undergoing changes. While in some cases the observed patterns fit well to received knowledge (for example, the belt of large-multiyear patches in the boreal where large fires are known to be the major driver of disturbances)[55,60], in others, the patterns do not align with our understanding of how unmanaged forests would behave. For instance, the small-isolated patches dominating in the remote forests of the Amazon (Fig. 2a) are consistent with the known structure of the lowland continental rainforest ecosystem, characterized by large continuous areas of mixed-age forests, with limited amounts of natural regrowth stands[47,61,62]. Also, the larger proportions of large-multiyear patches, compared with the intact forests of the African and Indomalayan realms (Supplementary Fig. 12b), are expected with the increasing vulnerability to wildfire and extreme weather events reported in the Amazon as a result of El Niño, climate stress and anthropogenic pressures[58]. However, in the Congo basin in Africa, the smaller rainforest fragments, dissected by road networks and encroaching farming, show an overall tendency towards large-multiyear patches (Fig. 2a), well above the typical small size of shifting agriculture[60,63]. While Amazonian and African rainforests differ

https://doi.org/10.1038/s41893-024-01450-3

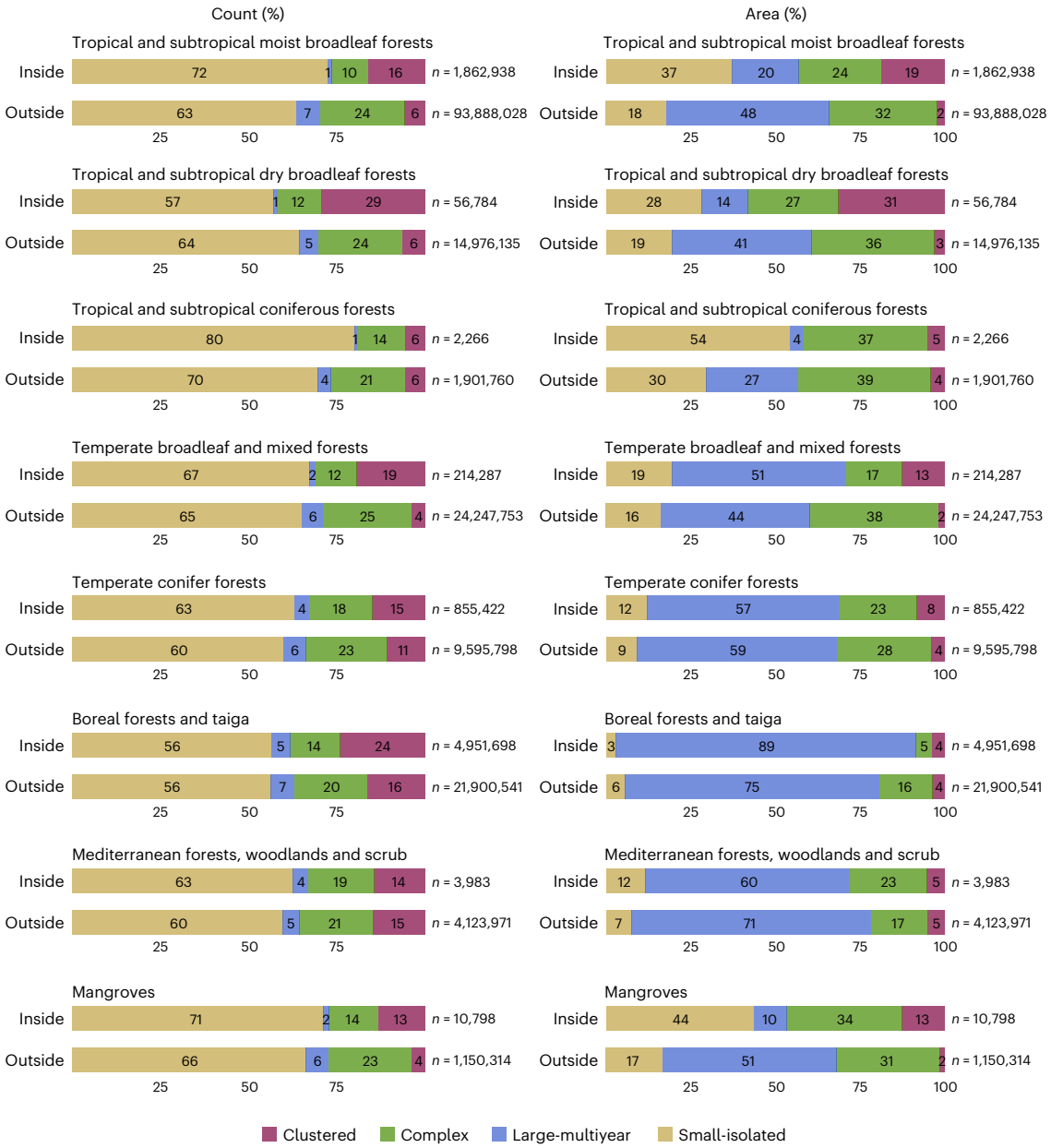

Fig. 3 | Proportion of disturbance patterns inside and outside intact forests by biome based on counts and areas. The total areas of disturbance patterns show that in the intact tropical moist broadleaf forests, the small-isolated and clustered patterns predominate, while large-multiyear patterns are minor.

in structure and composition[64], the broad characteristics of these forests remain similar[65] and the larger disturbance patches found imply that a fundamental change to the forest structure is underway. In tropical forests, small-isolated patches can positively influence biodiversity, as they contribute to increased light penetration in a moderate way and generate structural complexity within the environment, thus increasing habitat diversity and richness[66], whereas large-multiyear patches are likely to clear large areas, changing both the types of tree species that will repopulate them, with long-term implications for food sources and habitats[67,68]. Broad-scale maps of tree species functional strategies are not yet available across the tropics, but we hypothesize that a comparison of our maps with species life-history strategies would reveal large regions where the distribution of early and late successional species across the landscape is not consistent with the prevailing disturbance patch structure.

There are several instances in which a climatically and pedologically similar region is bisected by a marked change in dominant patch structure, for instance, the borders between Finland and Russia (Fig. 2b and Supplementary Fig. 4). All these cases are characterized by a shift in dominant patch characteristics from a relatively uniform structure across the country to a more varied regime. Finland has much simpler patch shapes than the neighbouring region of Russia, and those patches also tend to be more clustered in time. Such changes along country borders are indicative of how forest management practices have fundamentally altered the disturbance regimes. Forests in both Sweden and Finland are very intensively managed[69], and it is notable how the dominant cluster within the country is much more uniform than in their less intensively managed neighbours. Forests known to have little harvesting activity, such as the Amazon[47] or where natural disturbances are still the dominant regime, such as the northern Canadian boreal forest[12], tend to show much less uniform spatial patterns at the regional level. This has similarities with the process of biotic homogenization that has been reported as a result of transportation of species by humans[70] and is anticipated as a result of climate change[71,72].

https://doi.org/10.1038/s41893-024-01450-3

Fig. 4 | Proportions of dominant agents by forest biome for each disturbance pattern based on counts and areas. The 'other' category represents non-identified dominant drivers, which may include natural disturbances, such as biotic outbreaks and windthrow. The clustered pattern shows a distinct distribution among biomes, with a substantial association with fire in the boreal, Mediterranean and temperate conifer biomes, and an association with other drivers in the tropical coniferous biome. The large-multiyear pattern also shows a substantial association with fire and harvest, particularly in the boreal and Mediterranean biomes for the former and the tropical broadleaf biomes for the latter. Bars with values less than 1 are not labelled.

This suggests the hypothesis that regions with more uniform disturbance patch structures are both more biotically homogeneous and more inclined to biotic homogenization[73].

Counter to this idea of regional homogenization, however, we also found more diversity in patches at the landscape scale (that is, within the 0.1° grid cells) in intensively managed areas, including not just Finland and Sweden, but also much of Europe, southwestern United States and southern China (Fig. 2a)[20]. The higher patch diversity reflects a superposition of relatively regular harvest interventions and natural disturbance regimes. This will ultimately have a diversifying effect on forest landscape structure, relative to the natural state, but whether the increased habitat variability will result in higher diversity of flora and fauna will depend on the intensity of management (for example, the use of exotic monocultures and removal of deadwood) and its spatial composition and the traits of the species. A review of recent empirical studies has shown that higher patch structural diversity results in greater species diversity at the landscape scale[74].

Pervasive anthropogenic signature

This Analysis constitutes a comprehensive description of the characteristics of forest disturbances across the globe from a patch perspective. The patterns identified provide a new perspective on forest biogeography, revealing how the realized form of one of the key drivers of forest structure varies dramatically across the globe, emerging from the likely interplay of physical, biological and anthropogenic drivers. Four broad classes of disturbance patterns were identified integrating across patch areas, shapes, spatial arrangement and temporal continuity. These classes represented a similar fraction of disturbances across different forest biomes, but there was spatial variation in the dominant class within individual biomes. Variability within biomes emerges from both widespread anthropogenic modification of forests and natural variability within the broad classification of biomes, indicating that broad generalizations about disturbance patch structures by biome are probably inappropriate.

We found indications that human activities (harvest or small agriculture) may leave a consistent and uniform mark on landscapes, independently of the biome and regional climate, characterized by patches that are either complex or large and spread across multiple years. Such consistency would imply that human activities are leading towards a structural homogenization of the world's forests, with potential consequences on forest functions and the diversity of species they host. However, the increases in patch diversity in heavily managed ecosystems suggest that even when humans have enacted dramatic structural changes to forests, the characteristics of the natural disturbance regime are not entirely wiped out. Our results also suggest that natural agents, such as storms and fire, may leave similar structural signatures across regions assuming they are under similar bioclimatic conditions, as reported across protected forests under temperate and boreal climates[17,18].

The data we generated and combined for individual disturbance patches provide a rich dataset for further research, notably for quantifying disturbance regimes across regions, discriminating anthropogenic from natural processes and potentially elucidating the causal agents (for example, refs. 75,76). Such information on differences in disturbance characteristics between intact and non-intact forests can also provide a powerful reference for guiding the implementation of nature-based forest planning and management.

Methods

Tree cover loss data

We used the Landsat-derived GFC data version 1.6 to delineate tree cover loss patches between 2000 and 2018[10]. This dataset captures annually any complete or near-complete loss of woody vegetation that is taller than 5 m (considered as trees) and within a 1 arcsec resolution pixel (around 30 m at the equator). The loss detected is relative to 2000, whether the tree cover was natural or planted. The GFC data were processed using median observations from high-quality Landsat imagery acquired during the growing season between 2000 and 2018 and a bagged decision tree algorithm[10]. Years of tree cover loss were disaggregated by pixel using a set of heuristics derived from the maximum annual decline in both percentage tree cover and minimum growing season normalized vegetation difference index (NDVI)[10]. Thus, pixel values represent the year when the loss occurred the first time since 2000. Disturbances that follow this first loss (for example, due to seasonal agents, such as wildfire) are ignored. No initial canopy density threshold was applied while mapping the change (that is, losses in open-canopy forests and other treed vegetation communities are included). Disturbances occurring late in the year, after acquisition of the annual Landsat data, may be assigned to the following year.

At the global scale, the overall accuracy reported for the first version of the tree cover loss product is 99.6 (based on 1,500 sample blocks, 120 m in length per side)[10]. The prevalence of errors varies by biome and is equal to 13% for false positives (commission errors) and 12% for false negatives (omission errors)[49]. However, no uncertainty layer is provided in the data published for pixelwise quality filtering. Also, the validation of the loss classification did not include results from Landsat 8 images.

Projection

To calculate patch shape metrics accurately, we projected the global tree cover loss rasters with the Universal Transverse Mercator (UTM) projection system. The latter consists of a group of projections that are parametrized by geographic locations. These UTM zones span every 6° of longitude and are further subdivided every 8° of latitude to form a UTM grid zone[77]. The UTM projection is conformal, allowing the conservation of shapes and thus the retrieval of pixel connectedness[77]. Area distortions are negligible within the margins of a UTM zone, but accumulate more in higher latitudes because of more tiling (Supplementary Fig. 1). Splitting the global data by UTM grid zones also allowed optimizing computation time by parallelizing data processing among tiles. The UTM grid zone dataset was downloaded from the ESRI website[78] and consists of 1,201 tiles, among which 489 contained tree cover loss information (Supplementary Fig. 1). Tiling was performed in Google Earth Engine[79]. Exported tiles were reprojected by UTM grid zone at a resolution of 30 m using the ArcPy library from ArcGIS Desktop 10.7 (ref. 80) and Python 3.8 (ref. 81).

Pixel correction

To accurately retrieve the true shape and size of individual forest loss patches and at the same time identify patches that are growing over years, we applied, before patch delineation, a correction of the year assigned to the original tree cover loss pixels (Supplementary Fig. 2). The aim was to identify spatially and temporally contiguous pixels reflecting tree cover loss as a single composite patch. This allowed us to correct potential interannual splitting due to delayed detection resulting from the Landsat ETM+ Scan Line Corrector anomaly[82], cloud obstruction, events occurring late in the year (for example, December) or residual loss around patches. Grouping these tree cover loss areas together also enabled us to capture those processes that are moving and operating over multiple years, which manifest in our data as patches that are gradually growing outwards[83]. These include, among others, biotic outbreaks, plantation expansion with annual harvesting of neighbouring forests or cascading events, such as wind damage followed by insect infestations. The algorithm applied used R 4.3.1 (ref. 84) and C++11 (ref. 85) to identify loss pixels that are in consecutive years and adjoining each other. It then reassigned them to the most frequent year using the mode statistic at each iteration. Where there were equal frequencies (ties), the year with the lowest value was retained.

Patch delineation

We used the corrected tree cover loss rasters to delineate patches globally by tile. The delineation was conducted in R using an eight-cell (queen) neighbourhood rule. It was performed regardless of canopy density percentage, as our objective was to capture the spatial imprint left by a disturbance on the treed landscape. The minimum patch size was approximately 0.09 ha (30 m pixel resolution).

In total, 344,893,162 tree cover loss patches were identified for the period 2001–2018, including land use change. Individual patches with extreme values were checked by visual interpretation using aerial imagery in Google Earth Pro 7.3 (refs. 86,87 and Supplementary Fig. 6). The patch that has the largest area (221,025.5 ha) and also the longest perimeter (26,869,920 m) is a wildfire that occurred in 2002 in boreal eastern Siberia. The most elongated patch (0.995) is a road that was not large enough to be excluded with the ESA CCI Land Cover data[39]. The patch with the largest number of surrounding patches (4,155) is also a wildfire that occurred in Mediterranean Australia in 2010. The patch spanning the longest period (8 years) corresponds to a slash-and-burn agricultural expansion in Cambodia.

Limitations of the patch correction and delineation approach

A limitation of the patch correction applied with the majority vote (that is, most frequent year) is that it caps the size of growing patches after the number of new pixels (that is, years) to add becomes a minority. In fact, the merging of subsequent patches is chronologically unidirectional starting from 2001 and ending up until the number of new pixels to merge becomes smaller than the pixels already merged, which breaks the sequence with other potential temporally consecutive pixels, which can make the count of years (growth) smaller than it should be. It does, however, avoid the case in which a large patch continues to grow indefinitely by a few pixels each year, which would not be consistent with the intention of using this temporal metric to identify patches that grow substantially over multiple years (Supplementary Fig. 2b). Such cases of long serial merging are, in any case, rare in our database, as most patches that have been merged (count of years > 1) represent 8.17% of the global database (28,190,664 over 344,893,162 polygons), with a mean of 2.14 for the count of years of these merged patches. Composite patches counting more than 3 years represent only 1% of the database (354,539 polygons).

The gridding of global tree cover loss rasters with the UTM grid zones artificially split disturbance patches located at the edges of the UTM tiles, which may increase the number of patches identified and reduce their calculated sizes, thus affecting derived patch metrics. Before deploying the patch delineation globally, we tested on a smaller region whether a correction across tiles (for example, moving window) was needed. We selected a region susceptible to this artefact: the highly disturbed North American boreal biome, where patches tend to be larger and in higher numbers and thus more likely to be found at the edges of tiles. We found that the number of patches that were broken apart by the tiling there represented only 0.025% (6,197 polygons crossing the margins, over 24,315,498 polygons). We considered this proportion negligible and thus applied no corrections for this artefact.

Metrics calculation

To quantify patch structure, we considered several candidate metrics measuring magnitude (size and growth), shape complexity and context (spatio-temporal clustering) (Supplementary Table 1). Corrected patches were first polygonized using the ArcPy library in ArcGIS Server 1.7.1 (ref. 88). The geodesic area, perimeter and radius of the minimum circumscribing circle were then calculated. Shape indices[89] (that is, perimeter-to-area ratio, shape index, elongation index and fractal dimension index) were derived from these primary metrics. Patch growth was extracted during patch correction by counting the number of years composing the corrected patches. Patch context metrics were calculated within 5 km of the patch internal centroids using R and the UTM-projected rasters.

Isolating disturbances from deforestation

We used the ESA CCI Land Cover product[39] to isolate disturbances (temporary loss patches) from land use change (persistent loss patches caused by anthropogenic activities). As the resolution of ESA land cover is 10 times coarser than the GFC product (300 m versus 30 m), we excluded only large forest conversions that are at a scale detectable by the ESA product and considered smaller events as disturbances (including shifting agriculture and selective logging, which are small and generally non-permanent). Areas of large forest conversion were identified as pixels, classified as forests in 2000 (cover classes 50, 60, 61, 62, 70, 71, 72, 80, 81, 82, 90, 100, 160 and 170), which were changed to non-forest-related, assumed human-modified, covers at the end of the period studied (cover classes 10, 11, 20, 30, 110, 130 and 190, corresponding mainly to croplands, pasturelands and built-up areas). Corrected tree cover loss patches were then labelled as land use change if 10% of their area overlaps with these large forest conversion pixels. We increased the sensitivity to overlapping because, considering the coarse resolution of the land cover data (9 ha), we preferred to exclude a maximum of land-use-related patches and minimize cases in which conversion and disturbances were mixed to not obscure our conclusions with deforestation patterns. Thus, our approach excludes cases in which land use directly causes neighbouring disturbances, such as fire from land clearing spreading into nearby forests. We further conducted a sensitivity analysis experimenting with different thresholds (10%, 25% and 50%) and comparing how many patches were classified as land use across different biomes. To check the case of a fire from human activities spreading into intact forests, we took a subset of large patches (>1,000 ha), whose majority area is within intact forests, but their portion outside fulfil the land use attribution condition. The number of patches classified as land use with the 10% threshold and extending inside intact forests was very small (1 for the boreal forests and 6 for tropical moist forests) (Supplementary Table 3). This supported our decision to keep the 10% threshold.

Ensuring spatio-temporal consistency

After applying the patch correction algorithm, we observed an abrupt increase in mean patch sizes for 2015 onwards across all biomes (Supplementary Fig. 3). The GFC tree cover loss time series data are not consistent over time beyond 2012, as they have been affected by an increase in detection sensitivity, marked after 2015, due to the combined effects of adjustments in the classification algorithm, improvements in the Landsat instruments and increased image richness[90,91]. The increase in sensitivity concerns partial and short-term changes in tree cover, including residual loss and delayed tree mortality around disturbance patches. As these are more prevalent in the new GFC tree cover loss dataset, this led to more pixels being grouped together by our algorithm as a single patch, leading in turn to abruptly larger patches after 2014. We therefore focused our analysis on the years between 2002 and 2014, during which the mean corrected patch area remained stable (Supplementary Fig. 3), and considered the patch metrics derived during this period as viable indicators. Regarding the correction applied, we decided to keep the areas added to the composite patches beyond 2002–2014, as we consider them reflecting the full extent of the disturbance processes.

We expect that the spatial variability in Landsat data richness[13] would not affect our results as much as the temporal inconsistencies, as we are not using directly the year attribution of the loss in our analysis. In fact, we assume that any spatial bias would be minimized by the temporal flattening applied for delineating patches. In areas affected by a lack of observations due to cloud or snow obstruction, patches may be detected with a 1 or 2 year delay, but they should in most cases still be detected. If a patch is partially detected, the algorithm used to merge

contiguous patches will allow us to retrieve its true and realized size and shape by merging it with its other parts detected in the following years. However, in areas where regrowth may be fast enough to cover the patch entirely or partially before it is detected in the following years, this would result in patches delineated with a smaller size, fractured, or in a smaller number, with single-pixel disturbances probably missed. This situation is most likely to occur in dense-canopy rainforests, particularly in the tropics, where regrowth may be fast.

This being said, we consider that overall, there are sufficient usable observations over the period studied to minimize the errors described above and expect these would not affect our conclusions at regional and biome scales. This is all the more supported by the various patch types found across rainforests in the pantropical regions (for example, small-isolated and clustered in the Amazon, small-isolated inside intact forests and large-multiyear outside intact forests in Borneo), which agree more with the literature describing disturbances in these regions (for example, blowdowns in the Amazon, oil palm plantations in Indonesia) (Fig. 2a). Also, considering the Congolian lowland forests in western Africa, one of the regions with the least usable observations[13], we can retrieve similar patterns, with small-isolated and clustered patches inside the intact forests there and more complex multiyear patches outside the intact forests. We therefore conclude that our results and conclusions are robust to any variations in spatial consistency of disturbance classification errors.

Metrics selection and cluster analysis

We first selected the metrics that are meaningful for capturing the structural aspects considered: magnitude, complexity and clustering (Supplementary Table 1). We then assessed the correlation between these metrics to exclude those that are strongly multicollinear. This is needed to avoid conceptual redundancy between factors and consequent overweighting in the clustering, as well as to reduce dimensionality and thus data sparsity. We measured correlation using R and the Spearman method[92], as some metrics were severely skewed and thus not fulfilling the normality assumption. We set 0.75 as the threshold for the mean absolute correlation coefficient beyond which the metrics are considered multicollinear. We chose a high value for the threshold, as patch metrics were derived from each other and thus tend to be correlated, although reflecting subtle differences in structural traits. The area, perimeter, shape and fractal dimension indices showed high correlations (Supplementary Fig. 7). We thus excluded the perimeter and fractal dimension metrics from the clustering. However, we kept the area metric despite its multicollinearity, as we consider it an essential descriptor of patch types. We also preferred the shape metric over the perimeter-to-area ratio, as it is corrected for patch size differences. This also resulted in a balanced representation of complexity with two metrics for each conceptual class of magnitude, shape and context (Table 1). We then standardized the observations for each metric by subtracting the mean of the metric and dividing the result by the standard deviation. This allowed us to have equivalent variance among the variables and thus avoid building clusters only with the metrics having the highest amount of variation.

To identify natural grouping of patch structures, we used R to apply unsupervised clustering with *k*-means[40]. This method partitions data into a specific number of clusters by minimizing distances between observations and the centroid of clusters to which they are assigned[40]. We selected this algorithm for its ease in interpretation and implementation on large datasets. We specified Euclidean distances for measuring dissimilarities and 100 as the maximum number of iterations. For selecting the optimal number of clusters for the grouping, we tested numbers between 1 and 10 on samples of 10,000 patches randomly selected by forest ecobiomes and 50,000 patches globally. We checked the goodness of the clustering using silhouette coefficients and the Dunn index with 100 bootstraps. The optimal number of clusters varied substantially depending on regions and the patterns that dominate there. We decided to use four clusters, as it resulted in a stable and interpretable grouping, associated with substantially different metric means at the global scale, while also maximizing cluster separability and compactness (for the global sample, the average silhouette width = 0.42).

Ancillary data calculation

To explore linkages with environmental characteristics, we associated each patch with the following datasets:

1. Ecoregions, ecobiomes and biomes: Ecoregions2017[93] (polygons)
2. Forest intactness: Intact Forest Landscapes 2016[41] (polygons)
3. Forest types in 2000: ESA CCI Land Cover[39] (raster 300 m)
4. Fire: GFC Fire[58] (raster 30 m)
5. Drivers: dominant agents[60] (raster 10 km)
6. Forest landscape integrity index[56] (raster 300 m)
7. Elevation: JAXA ALOS DEM[94] (raster 30 m)
8. Countries: GADM[95] (polygons)

Ancillary rasters with a resolution smaller than 1 km were split with the UTM grid zones, reprojected accordingly and snapped to the extent of the projected disturbance rasters, so as to align with the patch pixels. Zonal statistics were applied using ArcPy. Each patch was attributed either the mean (elevation and forest landscape integrity index) or the most frequent value (ecoregions, forest types) of the ancillary data. A cover percentage threshold was used for attributing fire (25% of the patch area) and forest intactness (50%). For ancillary rasters with a resolution coarser than 1 km (that is, dominant agents), patches were assigned the values extracted at the centroid of the patch using R.

Mapping

To visualize the distribution of patch structural patterns, we built grids of patch statistics for every 0.1° grid cell. Statistics were summarized depending on the patch internal centroid using R. We quantified the relative importance of patterns based on the total count of patches and the associated total disturbance area. We used the Shannon–Wiener diversity index to measure the diversity of patterns, accounting for the evenness of their abundance and emphasizing rare types. Forest total areas were calculated per 0.1° grid cell, accounting only for tree cover with a canopy density greater than 10% as measured for 2000 in the GFC product. The raster was produced in Google Earth Engine and used to normalize disturbance patch counts per grid cell. Map rendering was performed in ArcGIS Desktop.

Reporting summary

Further information on research design is available in the Nature Portfolio Reporting Summary linked to this article.

Data availability

The produced patch metrics database is publicly available via Zenodo at https://doi.org/10.5281/zenodo.10108963 (ref. 96). Aggregated global maps of the patch metrics can be visualized in Google Earth Engine at https://ee-treemort-disturbances-nacil.projects.earthengine.app/view/patchmetrics2002-2014 and accessed from the asset 'projects/ee-treemort-disturbances-nacil/assets/PatchMetrics_Means_nonLU_2002-2014'. The database was derived from the Global Forest Change Tree Cover Loss Year dataset version 1.6 available at https://earthenginepartners.appspot.com/science-2013-global-forest/download_v1.6.html.

Code availability

The scripts used to produce the database and results are hosted in GitHub at https://github.com/N-Acil/GlobalForestDisturbances_PatchMetrics and in Google Earth Engine at https://code.earthengine.google.com/?accept_repo=users/NXA807/GlobalForestDisturbances_PatchMetrics.

References

1. Oliver, C. D. & Larson, B. A. *Forest Stand Dynamics, Update Edition* (Wiley, 1996).
2. Spies, T. & Turner, M. in *Maintaining Biodiversity in Forest Ecosystems* (ed. Hunter, M.) Ch. 4 (Cambridge Univ. Press, 1999); https://doi.org/10.1017/CBO9780511613029.006
3. Pugh, T. A. M. et al. Important role of forest disturbances in the global biomass turnover and carbon sinks. *Nat. Geosci.* **12**, 730–735 (2019).
4. Foster, D. R. et al. Landscape patterns and legacies resulting from large, infrequent forest disturbances. *Ecosystems* **1**, 497–510 (1998).
5. Heinselman, M. R. Fire in the virgin forests of the Boundary Waters Canoe Area, Minnesota. *Quat. Res.* **3**, 329–382 (1973).
6. Pugh, T. A. M. et al. Role of forest regrowth in global carbon sink dynamics. *Proc. Natl Acad. Sci. USA* **116**, 4382–4387 (2019).
7. Seidl, R. et al. Review: Searching for resilience: addressing the impacts of changing disturbance regimes on forest ecosystem services. *J. Appl. Ecol.* **53**, 120–129 (2016).
8. Franklin, J. F. & Forman, R. T. T. Creating landscape patterns by forest cutting: ecological consequences and principles. *Landsc. Ecol.* **1**, 5–18 (1987).
9. Norris, D. et al. Habitat patch size modulates terrestrial mammal activity patterns in Amazonian forest fragments. *J. Mammal.* **91**, 551–560 (2010).
10. Hansen, M. C. et al. High-resolution global maps of 21st-century forest cover change. *Science* **342**, 850–853 (2013).
11. Senf, C. & Seidl, R. Storm and fire disturbances in Europe: distribution and trends. *Glob. Change Biol.* **27**, 3605–3619 (2021).
12. White, J. et al. A nationwide annual characterization of 25 years of forest disturbance and recovery for Canada using Landsat time series. *Remote Sens. Environ.* **194**, 303–321 (2017).
13. Zhang, Y. et al. Mapping causal agents of disturbance in boreal and arctic ecosystems of North America using time series of Landsat data. *Remote Sens. Environ.* **272**, 112935 (2022).
14. Shikhov, A. N. Satellite-based analysis of the spatial patterns of fire- and storm-related forest disturbances in the Ural region, Russia. *Nat. Hazards* **97**, 283–308 (2019).
15. Goodbody, T. R. H. et al. Uncovering spatial and ecological variability in gap size frequency distributions in the Canadian boreal forest. *Sci. Rep.* **10**, 6069 (2020).
16. Sebald, J. et al. Human or natural? Landscape context improves the attribution of forest disturbances mapped from Landsat in central Europe. *Remote Sens. Environ.* **261**, 112502 (2021).
17. Seidl, R. et al. Globally consistent climate sensitivity of natural disturbances across boreal and temperate forest ecosystems. *Ecography* **43**, 967–978 (2020).
18. Sommerfeld, A. et al. Patterns and drivers of recent disturbances across the temperate forest biome. *Nat. Commun.* **9**, 4355 (2018).
19. Potapov, P. et al. The last frontiers of wilderness: tracking loss of intact forest landscapes from 2000 to 2013. *Sci. Adv.* **3**, e1600821 (2017).
20. Lesiv, M. et al. Global forest management data for 2015 at a 100 m resolution. *Sci. Data* **9**, 199 (2022).
21. Dyer, R. C. Remote sensing identification of tornado tracks in Argentina, Brazil and Paraguay. *Photogramm. Eng. Remote Sens.* **54**, 1429–1435 (1988).
22. Cannon, J. B. et al. Landscape-scale characteristics of forest tornado damage in mountainous terrain. *Landsc. Ecol.* **31**, 2097–2114 (2016).
23. Shikhov, A. N. & Chernokulsky, A. V. A satellite-derived climatology of unreported tornadoes in forested regions of northeast Europe. *Remote Sens. Environ.* **204**, 553–567 (2018).
24. Xi, W. & Peet, R. K. in *Recent Hurricane Research—Climate, Dynamics, and Societal Impacts* (ed. Lupo, A.) Ch. 27 (IntechOpen, 2011); https://doi.org/10.5772/16167
25. Senf, C. et al. Remote sensing of forest insect disturbances: current state and future directions. *Int. J. Appl. Earth Obs. Geoinf.* **60**, 49–60 (2017).
26. Scholter, R. C. et al. Overwintering fires in boreal forests. *Nature* **593**, 399–404 (2021).
27. Pimont, F. et al. Coupled slope and wind effects on fire spread with influences of fire size: a numerical study using FIRETEC. *Int. J. Wildland Fire* https://doi.org/10.1071/WF11122 (2012).
28. Popović, Z. et al. Tree species flammability based on plant traits: a synthesis. *Sci. Total Environ.* **800**, 149625 (2021).
29. Hennon, P. E. et al. A framework to evaluate climate effects on forest tree diseases. *For. Pathol.* https://doi.org/10.1111/efp.12649 (2020).
30. Schelhaas, M.-J. et al. Natural disturbances in the European forests in the 19th and 20th centuries. *Glob. Change Biol.* **9**, 1620–1633 (2003).
31. Seidl, R. et al. Unravelling the drivers of intensifying forest disturbance regimes in Europe. *Glob. Change Biol.* **17**, 2842–2852 (2011).
32. Murcia, C. Edge effects in fragmented forests: implications for conservation. *Trends Ecol. Evol.* **10**, 58–62 (1995).
33. Daniels, M. K. & Larson, E. R. Effects of forest windstorm disturbance on invasive plants in protected areas of southern Illinois, USA. *J. Ecol.* **108**, 199–211 (2019).
34. Saunders, D. et al. Biological consequences of ecosystem fragmentation: a review. *Conserv. Biol.* **5**, 18–32 (1991).
35. De Frenne, P. et al. Forest microclimates and climate change: importance drivers and future research agenda. *Glob. Change Biol.* **27**, 2279–2297 (2021).
36. Charbonneau, N. C. & Fahrig, L. Influence of canopy cover and amount of open habitat in the surrounding landscape on proportion of alien plant species in forest sites. *Ecoscience* **11**, 278–281 (2004).
37. Daskalova, G. N. et al. Landscape-scale forest loss as a catalyst of population and biodiversity change. *Science* **368**, 1341–1347 (2020).
38. Hagmann, R. K. et al. Contemporary wildfires further degrade resistance and resilience of fire-excluded forests. *For. Ecol. Manage.* **506**, 119975 (2022).
39. Defourny, P. et al. *ESA, Land Cover CCI Product User Guide—Version 2.0* (ESA, 2017).
40. Lloyd, S. P. Least squares quantization in PCM. *IEEE Trans. Inf. Theory* **28**, 129–137 (1982).
41. Potapov, P. et al. Mapping the world's intact forest landscapes by remote sensing. *Ecol. Soc.* **13**, 51 (2008).
42. Rahman, M. H. et al. Oil palm and rubber-driven deforestation in Indonesia and Malaysia (2000-2021) and efforts toward zero deforestation commitments. Preprint at *Research Square* https://doi.org/10.21203/rs.3.rs-2945587/v1 (2023).
43. Xu, Y. et al. Annual oil palm plantation maps in Malaysia and Indonesia from 2001 to 2016. *Earth Syst. Sci. Data* **12**, 847–867 (2020).
44. Rackham, O. *The History of the Countryside: The Full Fascinating Story of Britain's Landscape* (J. M. Dent, 1986).
45. Watts, K. et al. *Evaluating Biodiversity in Fragmented Landscapes* (Forestry Commission, 2005); https://cdn.forestresearch.gov.uk/2022/02/fcin073-6.pdf
46. Shannon, C. E. A mathematical theory of communication. *Bell Syst. Tech. J.* **27**, 379–423 (1948).
47. Espírito-Santo, F. D. B. et al. Size and frequency of natural forest disturbances and the Amazon forest carbon balance. *Nat. Commun.* **5**, 3434–3434 (2014).
48. Chambers, J. Q. et al. The steady-state mosaic of disturbance and succession across an old-growth central amazon forest landscape. *Proc. Natl Acad. Sci. USA* **110**, 3949–3954 (2013).

49. Global Forest Watch How accurate is accurate enough? Examining the GLAD global tree cover change data (Part 1). *World Resources Institute* https://www.globalforestwatch.org/blog/data-and-research/how-accurate-is-accurate-enough-examining-the-glad-global-tree-cover-change-data-part-1/ (2015).
50. Negron-Juarez, R. et al. Vulnerability of Amazon forests to storm-driven tree mortality. *Environ. Res. Lett.* https://doi.org/10.1088/1748-9326/aabe9f (2018).
51. Espírito-Santo, F. D. B. et al. Storm intensity and old-growth forest disturbances in the Amazon region. *Geophys. Res. Lett.* https://doi.org/10.1029/2010GL043146 (2010).
52. Baguskas, S. A. et al. Evaluating spatial patterns of drought-induced tree mortality in a coastal California pine forest. *For. Ecol. Manage.* **315**, 43–53 (2014).
53. Senf, C. & Seidl, R. Natural disturbances are spatially diverse but temporally synchronized across temperate forest landscapes in Europe. *Glob. Change Biol.* **24**, 1201–1211 (2018).
54. Turner, M. G. et al. Predicting the spread of disturbance across heterogeneous landscapes. *Oikos* **55**, 121–129 (1989).
55. Andela, N. et al. The Global Fire Atlas of individual fire size, duration, speed and direction. *Earth Syst. Sci. Data* **11**, 529–552 (2019).
56. Grantham, H. S. et al. Anthropogenic modification of forests means only 40% of remaining forests have high ecosystem integrity. *Nat. Commun.* **11**, 5978 (2020).
57. Sharma, A. et al. Long-term effects of catastrophic wind on southern US coastal forests: lessons from a major hurricane. *PLoS ONE* **16**, e0243362 (2021).
58. Tyukavina, A. et al. Global trends of forest loss due to fire from 2001 to 2019. *Front. Remote Sens.* https://doi.org/10.3389/frsen.2022.825190 (2022).
59. Cannon, J. B. et al. A review and classification of interactions between forest disturbance from wind and fire. *For. Ecol. Manag.* **406**, 381–390 (2017).
60. Curtis, P. G. et al. Classifying drivers of global forest loss. *Science* **361**, 1108–1111 (2018).
61. Pickett, S. T. & White, P. S. *The Ecology of Natural Disturbance and Patch Dynamics* (Academic Press, 1985).
62. Denslow, J. S. Tropical rainforest gaps and tree species diversity. *Annu. Rev. Ecol. Syst.* **18**, 431–451 (1987).
63. Tyukavina, A. et al. Congo Basin forest loss dominated by increasing smallholder clearing. *Sci. Adv.* **4**, eaat2993 (2018).
64. Malhi, Y. et al. African rainforests: past, present and future. *Philos. Trans. R. Soc. B* **368**, 20120312 (2013).
65. Primack, R. B. & Corlett, R. T. *Tropical Rain Forests: An Ecological and Biogeographical Comparison* (John Wiley & Sons, 2011).
66. Pöpperl, F. & Seidl, R. Effects of stand edges on the structure functioning and diversity of a temperate mountain forest landscape. *Ecosphere* **12**, e03692 (2021).
67. Poorter, L. et al. Wet and dry tropical forests show opposite successional pathways in wood density but converge over time. *Nat. Ecol. Evol.* **3**, 928–934 (2019).
68. Turner, M. G. & Dale, V. H. Comparing large, infrequent disturbances: what have we learned? *Ecosystems* https://doi.org/10.1007/s100219900045 (1998).
69. Siiskonen, H. et al. From economic to environmental sustainability: the forest management debate in 20th century Finland and Sweden. *Environ. Dev. Sustain.* **15**, 1323–1336 (2013).
70. Daru, B. H. et al. Widespread homogenization of plant communities in the Anthropocene. *Nat. Commun.* **12**, 6983 (2021).
71. Zwiener, V. P. et al. Climate change as a driver of biotic homogenization of woody plants in the Atlantic Forest. *Glob. Ecol. Biogeogr.* **27**, 298–309 (2017).
72. Borderieux, J. et al. Extinction drives recent thermophilization but does not trigger homogenization in forest understorey. *Nat. Ecol. Evol.* **8**, 695–704 (2024).
73. Haslem, A. et al. Landscape properties mediate the homogenization of bird assemblages during climatic extremes. *Ecology* **96**, 3165–3174 (2015).
74. Fahrig, L. Why do several small patches hold more species than few large patches? *Glob. Ecol. Biogeogr.* **29**, 615–628 (2020).
75. Kennedy, R. E. et al. Attribution of disturbance change agent from Landsat time-series in support of habitat monitoring in the Puget Sound region, USA. *Remote Sens. Environ.* **166**, 271–285 (2015).
76. Shimizu, K. et al. Attribution of disturbance agents to forest change using a Landsat time series in tropical seasonal forests in the Bago mountains Myanmar. *Forests* https://doi.org/10.3390/f8060218 (2017).
77. ESRI Universal transverse mercator. *ArcMap* https://desktop.arcgis.com/en/arcmap/10.7/map/projections/universal-transverse-mercator.htm (2019).
78. ESRI World UTM grid. *ArcGIS Hub* https://hub.arcgis.com/datasets/esri::world-utm-grid/about (2018).
79. Gorelick, N. et al. Google Earth Engine: planetary-scale geospatial analysis for everyone. *Remote Sens. Environ.* **202**, 18–27 (2017).
80. ArcGIS Desktop, version 10.7 (ESRI, 2018).
81. Python Language Reference, version 3.8 (Python Software Foundation, 2021); http://www.python.org
82. USGS & NASA *Preliminary Assessment of the Value of Landsat 7 ETM+ SLC-off Data* (USGS, 2018); https://www.usgs.gov/media/files/preliminary-assessment-value-landsat-7-etm-slc-data
83. Krüger, K. et al. Gap expansion is the dominant driver of canopy openings in a temperate mountain forest landscape. *J. Ecol.* **112**, 1501–1515 (2024).
84. R Core Team. *R: A Language and Environment for Statistical Computing* http://www.R-project.org/ (R Foundation for Statistical Computing, 2021).
85. ISO/IEC *ISO/IEC 14882:2011: Programming Languages—C++* (International Organization for Standardization, 2012); https://www.iso.org/standard/50372.html
86. Google Earth Pro Desktop, version 7.3 (Google, 2023); https://www.google.com/intl/en_uk/earth/versions/
87. Google, CNES/Airbus, Landsat/Copernicus & Maxar Technologies Google Earth Pro Imagery, map data (2020).
88. ArcGIS Server, version 1.7.1 (ESRI, 2020).
89. McGarigal, K., Ene, E. & Cushman, S. FRAGSTATS v4: spatial pattern analysis program for categorical and continuous maps (2012); https://www.fragstats.org
90. Palahí, M. et al. Concerns about reported harvests in European forests. *Nature* **592**, E15–E17 (2021).
91. Weisse, M. & Potapov, P. Assessing trends in tree cover loss over 20 years of data. *Global Forest Watch* https://www.globalforestwatch.org/blog/data-and-research/tree-cover-loss-satellite-data-trend-analysis/ (2021).
92. Spearman, C. The proof and measurement of association between two things. *Am. J. Psychol.* **15**, 72–101 (1904).
93. Dinerstein, E. et al. An ecoregion-based approach to protecting half the terrestrial realm. *Bioscience* **67**, 534–545 (2017).
94. Tadono, T. et al. Precise global DEM generation by ALOS PRISM. *ISPRS Ann. Photogramm. Remote Sens. Spatial Inf. Sci.* **II-4**, 71–76 (2014); https://doi.org/10.5194/isprsannals-II-4-71-2014
95. Global Administrative Areas (GADM) *GADM Database of Global Administrative Areas (Version 3.6)* (2018, accessed 6 May 2018); https://gadm.org
96. Acil, N. et al. Patch metrics and landscape patterns of forest disturbances at the beginning of the 20th century. Version 1.0. *Zenodo* https://doi.org/10.5281/zenodo.10108963 (2023).

Acknowledgements
We thank P. Potapov for his quick and fulsome clarifications regarding the functioning of the algorithms behind the GFC product. We also thank J. Sebald for his insightful inputs during the discussions for developing the patch correction and clustering metrics. We further thank the team of Google Earth Engine and the University of Birmingham's High Performance Computing service, BlueBEAR, for providing and maintaining such powerful computation systems. This project was funded by the European Research Council (ERC) under the European Union's Horizon 2020 research and innovation programme (grant agreement number 758873, TreeMort). N.A. was also financially supported by the Natural Environment Research Council (NERC, NE/R016518/1) and the ESA BIOMASS CCI+. The contribution of S.S. was funded by European Union's Horizon 2020 research and innovation programme under the Marie Skłodowska-Curie grant agreement number 895158 (ForMMI). This paper is a contribution to the strategic research areas BECC and MERGE funded by the Swedish government and the Nature-Based Future Solutions profile area at Lund University.

Author contributions
N.A., T.A.M.P., J.P.S. and S.S. conceived the study. C.S. developed the algorithms for correcting patches and measuring their clustering over time and space. N.A. adapted and optimized the correction algorithms to be run on global data. N.A. conducted the geospatial and statistical analyses in consultation with T.A.M.P., J.P.S. and S.S. N.A. and T.A.M.P. co-wrote the paper, with extensive feedback and inputs from J.P.S., S.S. and C.S.

Competing interests
The authors declare no competing interests.

Additional information
Supplementary information The online version contains supplementary material available at https://doi.org/10.1038/s41893-024-01450-3.

Correspondence and requests for materials should be addressed to Nezha Acil.

Peer review information *Nature Sustainability* thanks Jiajia Liu and the other, anonymous, reviewer(s) for their contribution to the peer review of this work.

nature portfolio

Corresponding author(s): Nezha Acil

Last updated by author(s): Jul 30, 2024

Reporting Summary

Nature Portfolio wishes to improve the reproducibility of the work that we publish. This form provides structure for consistency and transparency in reporting. For further information on Nature Portfolio policies, see our Editorial Policies and the Editorial Policy Checklist.

Statistics

For all statistical analyses, confirm that the following items are present in the figure legend, table legend, main text, or Methods section.

n/a	Confirmed
☐	☒ The exact sample size (*n*) for each experimental group/condition, given as a discrete number and unit of measurement
☒	☐ A statement on whether measurements were taken from distinct samples or whether the same sample was measured repeatedly
☒	☐ The statistical test(s) used AND whether they are one- or two-sided *Only common tests should be described solely by name; describe more complex techniques in the Methods section.*
☐	☒ A description of all covariates tested
☐	☒ A description of any assumptions or corrections, such as tests of normality and adjustment for multiple comparisons
☐	☒ A full description of the statistical parameters including central tendency (e.g. means) or other basic estimates (e.g. regression coefficient) AND variation (e.g. standard deviation) or associated estimates of uncertainty (e.g. confidence intervals)
☒	☐ For null hypothesis testing, the test statistic (e.g. *F*, *t*, *r*) with confidence intervals, effect sizes, degrees of freedom and *P* value noted *Give P values as exact values whenever suitable.*
☒	☐ For Bayesian analysis, information on the choice of priors and Markov chain Monte Carlo settings
☒	☐ For hierarchical and complex designs, identification of the appropriate level for tests and full reporting of outcomes
☒	☐ Estimates of effect sizes (e.g. Cohen's *d*, Pearson's *r*), indicating how they were calculated

Our web collection on statistics for biologists contains articles on many of the points above.

Software and code

Policy information about availability of computer code

Data collection	Google Earth Engine, Google Earth Pro 7.3
Data analysis	Google Earth Engine, ArcGIS Desktop 10.7, ArcGIS Server 1.7.1, Python 3.8, R 4.3.1, C++11

For manuscripts utilizing custom algorithms or software that are central to the research but not yet described in published literature, software must be made available to editors and reviewers. We strongly encourage code deposition in a community repository (e.g. GitHub). See the Nature Portfolio guidelines for submitting code & software for further information.

Data

Policy information about availability of data

All manuscripts must include a data availability statement. This statement should provide the following information, where applicable:

- Accession codes, unique identifiers, or web links for publicly available datasets
- A description of any restrictions on data availability
- For clinical datasets or third party data, please ensure that the statement adheres to our policy

Data availability: The produced patch metrics database is publicly available in Zenodo (10.5281/zenodo.10108963). Aggregated global maps of the patch metrics can be visualised in the Google Earth Engine application https://ee-treemort-disturbances-nacil.projects.earthengine.app/view/patchmetrics2002-2014 and accessed in the asset "projects/ee-treemort-disturbances-nacil/PatchMetrics_Means_nonLU_2002-2014/". The database was derived from the Global Forest Change Tree Cover Loss Year dataset version 1.6 available at https://earthenginepartners.appspot.com/science-2013-global-forest/download_v1.6.html.

Code availability:
The scripts used to produce the database and results are hosted in GitHub (https://github.com/N-Acil/GlobalForestDisturbances_PatchMetrics) and Google Earth Engine (https://code.earthengine.google.com/?accept_repo=users/NXA807/ GlobalForestDisturbances_PatchMetrics).

Human research participants

Policy information about studies involving human research participants and Sex and Gender in Research.

Reporting on sex and gender	N/A
Population characteristics	N/A
Recruitment	N/A
Ethics oversight	N/A

Note that full information on the approval of the study protocol must also be provided in the manuscript.

Field-specific reporting

Please select the one below that is the best fit for your research. If you are not sure, read the appropriate sections before making your selection.

☐ Life sciences ☐ Behavioural & social sciences ☒ Ecological, evolutionary & environmental sciences

For a reference copy of the document with all sections, see nature.com/documents/nr-reporting-summary-flat.pdf

Ecological, evolutionary & environmental sciences study design

All studies must disclose on these points even when the disclosure is negative.

Study description	The study identifies and characterises prominent landscape patterns in forest disturbances at the global-scale using metrics reflecting disturbance structure in terms of magnitude, complexity and context.
Research sample	The study focuses on forest disturbance patches. We consider as forest disturbance any loss in tree cover identifiable with Landsat-derived data, excluding large land use changes, but including temporary anthropogenic activities (i.e. harvest and shifting agriculture).
Sampling strategy	The data collected and analysed cover the entire population of forest disturbance patches, as captured by Landsat sensors and detected by the Global Forest Change algorithm.
Data collection	Forest disturbance data are derived from an existing Landsat-based Global Forest Change tree cover loss database (Hansen et al, 2013). Ancillary data are also derived from other existing remote sensing databases cited in the manuscript.
Timing and spatial scale	Data were processed at 30m spatial resolution at the global scale on an annual basis. The initial period considered covered 2001-2018.
Data exclusions	Years 2001 and 2015-2018 were excluded to minimise inconsistencies in time series data.
Reproducibility	*Describe the measures taken to verify the reproducibility of experimental findings. For each experiment, note whether any attempts to repeat the experiment failed OR state that all attempts to repeat the experiment were successful.*
Randomization	*Describe how samples/organisms/participants were allocated into groups. If allocation was not random, describe how covariates were controlled. If this is not relevant to your study, explain why.*
Blinding	*Describe the extent of blinding used during data acquisition and analysis. If blinding was not possible, describe why OR explain why blinding was not relevant to your study.*

Did the study involve field work? ☐ Yes ☒ No

Reporting for specific materials, systems and methods

We require information from authors about some types of materials, experimental systems and methods used in many studies. Here, indicate whether each material, system or method listed is relevant to your study. If you are not sure if a list item applies to your research, read the appropriate section before selecting a response.

Materials & experimental systems

n/a	Involved in the study
☒	☐ Antibodies
☒	☐ Eukaryotic cell lines
☒	☐ Palaeontology and archaeology
☒	☐ Animals and other organisms
☒	☐ Clinical data
☒	☐ Dual use research of concern

Methods

n/a	Involved in the study
☒	☐ ChIP-seq
☒	☐ Flow cytometry
☒	☐ MRI-based neuroimaging